Mon. Not. R. Astron. Soc. **394,** 633–640 (2009) doi:10.1111/j.1365-2966.2008.14329.x

Imprints of recoiling massive black holes on the hot gas of early-type galaxies

B. Devecchi,[1]★ E. Rasia,[2]† M. Dotti,[3] M. Volonteri[3] and M. Colpi[1]

[1]*Dipartimento di Fisica G. Occhialini, Università degli Studi di Milano Bicocca, Piazza della Scienza 3, 20126 Milano, Italy*
[2]*Department of Physics, University of Michigan, Ann Arbor, MI 48109, USA*
[3]*Department of Astronomy, University of Michigan, Ann Arbor, MI 48109, USA*

Accepted 2008 December 4. Received 2008 November 5; in original form 2008 May 15

ABSTRACT

Anisotropic gravitational radiation from a coalescing black hole (BH) binary is known to impart recoil velocities of up to $\sim$1000 km s^{-1} to the remnant BH. In this context, we study the motion of a recoiling BH inside a galaxy modelled as a Hernquist sphere, and the signature that the hole imprints on the hot gas, using *N*-body/smoothed particle hydrodynamics simulations. Ejection of the BH results in a sudden expansion of the gas ending with the formation of a gaseous core, similarly to what is seen for the stars. A cometary tail of particles bound to the BH is initially released along its trail. As the BH moves on a return orbit, a nearly spherical swarm of hot gaseous particles forms at every apocentre: this feature can live up to $\approx 10^8$ years. If the recoil velocity exceeds the sound speed initially, the BH shocks the gas in the form of a Mach cone in density near each supersonic pericentric passage. We find that the X-ray fingerprint of a recoiling BH can be detected in *Chandra* X-ray maps out to a distance of Virgo. For exceptionally massive BHs, the Mach cone and the wakes can be observed out to a few hundred of milliparsec. The detection of the Mach cone is of twofold importance as it can be a probe of high-velocity recoils, and an assessment of the scatter of the $M_{\rm BH} - M_{\rm bulge}$ relation at large BH masses.

Key words: black hole physics – gravitational waves – hydrodynamics – methods: numerical – galaxies: nuclei – X-rays: galaxies.

1 INTRODUCTION

Today, black holes (BHs) with masses in excess of $10^6\,{\rm M}_\odot$ appear to be ubiquitous in bright galaxies. Richstone et al. (1998), Decarli et al. (2007) and scaling relations between the BH mass and the underlying galaxy indicate unambiguously that BHs evolve in symbiosis with their hosts (Ferrarese & Merritt 2000; Gebhardt et al. 2000; Hopkins et al. 2006).

According to the current paradigm of structure formation, galaxies often interact and merge as their dark matter haloes assemble in a hierarchical fashion, and the BHs, incorporated through mergers, are expected to grow, evolve and *pair* with other BHs (Volonteri, Haardt & Madau 2003). The formation of supermassive BH pairs thus appears to be an inevitable and natural consequence of galaxy assembly.

In our local universe, the dual radio source 3C 75, at the centre of Abell 400, is a clear, albeit rare, example of BH pairing as it hosts two massive BHs displaying prominent radio jets (Owen et al. 1985). *Chandra* observations of 3C 75 have revealed the occurrence of two active nuclei at a projected separation of 7 kpc (Hudson et al. 2006), providing first evidence of their current coupling. An even more remarkable, and still unique, example is the case of the elliptical galaxy 0402+369 (Rodriguez et al. 2006). Very long baseline interferometry observations highlighted the presence of two compact variable, flat-spectrum radio sources at a projected separation of only 7 pc, suggesting that the two massive BHs that power the radio emission form a *binary*. These two cases indicate that BH pairing occurs and proceeds from the large scale of a merger (up to 100 kpc) down to the scale where the BHs form a binary in close Keplerian relative orbit (of a few parsec). In the interaction with the stars (Milosavljević & Merritt 2001; Yu 2002; Merritt & Milosavljević 2005; Berczik et al. 2006; Sesana, Haardt & Madau 2007) and/or gas (Armitage & Natarajan 2002; Escala et al. 2004, 2005; Dotti, Colpi & Haardt 2006; Dotti et al. 2007; Mayer et al. 2007) that surround the binary, the BHs lose orbital angular momentum, and if the process continues down to a scale of a few milliparsec, gravitational wave emission drives the BH in-spiral down to coalescence, causing the formation of a heavier *remnant* BH.

Recently, a major breakthrough in numerical relativity has allowed for the first time to trace the BH binary evolution down to coalescence (Pretorius 2007), in the *strong-field* regime imposed

★E-mail: bernadetta.devecchi@mib.infn.it
†Chandra fellow.

by general relativity under arbitrary conditions (Favata et al. 2004; Baker et al. 2007, 2008; Bruegmann et al. 2008; Campanelli et al. 2007a,b; Herrmann et al. 2007a,b,c; Koppitz et al. 2007). These studies have revealed that spinning BHs emit an anisotropic beam of gravitational radiation, and in response to this asymmetry the remnant BH receives a *recoil* (due to linear momentum conservation) that can displace it from the central parts of the galaxy. In more detail, BHs with similar masses and spin vectors in non-generic alignments relative to the orbit produce anisotropic patterns of radiation via spin–orbit coupling that lead to recoil velocities $v_{\rm rec}$ in the range of $\lesssim$200 to 2000 km s^{-1}, and for particular spin–orbit configurations to a recoil as high as 4000 km s^{-1} (Campanelli et al. 2007a,b; Schnittman & Buonanno 2007; Baker et al. 2008). These 'natal kicks' are in the range of the typical dispersion/rotation velocities of galaxies or even higher, so that the remnant BH can either be significantly displaced away from the galactic centre where the merger occurred or be ejected when $v_{\rm rec}$ exceeds the escape speed from the galaxy (typically of $\sim$1000 km s^{-1} for massive galaxies).

Both a BH that remains and a BH that escapes can leave a 'sign' on the underlying galaxy with observable consequences. As an example, a BH ejected from its host galaxy can carry a punctuated accretion disc that lights the BH on, as an active X-ray source, eventually deprived of its underlying galaxy (Loeb 2007). Can a BH retained in the galaxy carry other observable features? This is the question that we address in this paper.

A kicked BH, retained inside the host galaxy, moves along a radially elongated orbit; it both explores the galaxy periphery and crosses the centre a few times, periodically. Dynamical friction against stars and gas causes its radial orbit to decay over a timescale that depends on the recoil velocity and underlying background density.

The BH-damped oscillatory motion, in a pure stellar background, has been investigated by a number of authors (Boylan-Kolchin, Ma & Quataert 2004; Merritt et al. 2004; Gualandris & Merritt 2007). After an early phase of braking under the action of dynamical friction and a number of recursive passages across the centre of the galaxy, the orbital decay causes the motion of the BH to be confined into its gravitational influence radius. From this point on, the BH starts oscillating together with the core around the common centre of mass, and it eventually reaches thermal equilibrium with the stars when the oscillations decay down to the Brownian level (Gualandris & Merritt 2007).

The interaction of the massive BH with stars can have significant consequences on the underlying equilibrium (Boylan-Kolchin et al. 2004; Merritt et al. 2004; Gualandris & Merritt 2007), the most interesting being the formation of a *stellar core*. As pointed out by Boylan-Kolchin et al. (2004), the instantaneous removal of the BH from the galaxy centre, at the time of its ejection, causes a sudden decrease in the gravitational potential so that the stellar component is driven away from virial equilibrium and expands. In addition, when the BH returns to the centre, it transfers orbital kinetic energy into the background under the action of dynamical friction, and this energy deposition causes further stellar expansion.

In this paper, we address a complementary problem that is the effect that a recoiling BH has on the hot gaseous component of an early-type galaxy host. Local temperature and density perturbations excited by the supermassive BH while it is travelling across the galaxy are expected to lead to observable changes of the bremsstrahlung emission. We will specifically address the following issues: (i) how the structural properties of the gas in the galaxy are modified by the ejection of the BH and its orbital decay; (ii) which signatures the BH motion imprints on the gas and (iii) the prospects for detection of these signatures by X-ray telescope such as *Chandra*.

For this study, we perform a suite of eight simulations of gas-rich elliptical galaxies, where BHs are ejected with different recoil velocities. The BH mass, $M_{\rm BH}$, scales with the host mass according to the observed correlation (Häring & Rix 2004). Since this correlation has an intrinsic scatter of at least 0.3 dex (see Lauer et al. 2007; Tundo et al. 2007 for a discussion of the scatter of the correlations at large BH masses), we also study the case of an overmassive BH with a mass a factor of 3 larger than that predicted by the best-fitting value of the $M_{\rm BH} - M_{\rm bulge}$ relation in Häring & Rix (2004).

The outline of this paper is as follows. In Section 2, we introduce the physical model used in our simulations. In Section 3, we describe the changes in time of the density and temperature induced by the ejected BH, inferred considering different recoil velocities, and for a BH mass following the $M_{\rm BH} - M_{\rm bulge}$ relation and its scatter. In Section 4, we explore the BH detectability with *Chandra*. In Section 5, we discuss our results.

2 SIMULATIONS

We perform our simulations using the *N*-body/smoothed particle hydrodynamics code GADGET (Springel, Yoshida & White 2001). The elliptical galaxies are modelled as a Hernquist sphere (Hernquist 1990) with scale radius a and total mass $M_{\rm tot}$. The mass density, cumulative mass profile and escape velocity are given by

$$\rho(r) = \frac{M_{\rm tot}}{2\pi}\frac{a}{r(r+a)^3} \tag{1}$$

$$M(r) = M_{\rm tot}\frac{r^2}{(r+a)^2} \tag{2}$$

$$v_{\rm esc} = (2GM_{\rm tot}/a)^{1/2}. \tag{3}$$

The total mass of the galaxy is $M_{\rm tot} = 10^{12}\,{\rm M}_\odot$, with a gas fraction $f_{\rm gas} \equiv M_{\rm gas}/M_{\rm tot} = 0.1$; the gas follows the same density profile of the stellar component. We explore two different scale radii: a equal to 4 and 8 kpc, and two different BH masses, 2 and $6 \times 10^9\,{\rm M}_\odot$ (see Table 1). The lightest BH follows the $M_{\rm BH} - M_{\rm bulge}$ relation as in Häring & Rix (2004), while the heaviest explores the scatter at high BH masses (Lauer et al. 2007; Tundo et al. 2007), where we expect the imprints of the recoils to be the largest.

For the collisionless component, we use 10^5 particles with a gravitational softening of 100 pc to prevent numerical collisional relaxation. In the runs with the light (heavy) BH, we use 2×10^6 (10^6) gaseous particles with softening $h_{\rm gas} = 10$ (50) pc; the number of gas particles used to average the hydrodynamical properties is 40, so that our mass resolution is $\approx 2 \times 10^7\,{\rm M}_\odot$ ($10^7\,{\rm M}_\odot$). Each gaseous particle is evolved along a polytrope $P \propto \rho^\gamma$ with $\gamma = 5/3$, corresponding to adiabatic evolution of an ideal gas. Compressional work and shock heating are included in the energy equation. The gravitational softening of the BH equals that of the gas, $h_{\rm BH} = h_{\rm gas}$. We ensure that the dynamical influence of the hole on the gas is resolved by checking that $h_{\rm BH} \ll r_{\rm inf} \simeq a\,(2\,M_{\rm BH}/M_{\rm tot})^{1/2}$. Here, the influence radius, $r_{\rm inf}$, is defined as the distance from the galaxy centre that encloses a total mass equal to $2\,M_{\rm BH}$. For the less massive BH:

$$r_{\rm inf} \simeq 253\,\left(\frac{a}{4\,{\rm kpc}}\right)\left(\frac{M_{\rm BH}}{2\times10^9\,{\rm M}_\odot}\frac{10^{12}\,{\rm M}_\odot}{M_{\rm tot}}\right)^{1/2}\,{\rm pc}. \tag{4}$$

We set the initial condition for the BH plus galaxy system following the prescription by Hernquist (1993), and evolve the equilibrium

Table 1. List of the simulations: label of the run; BH mass in unit of $10^9\,M_\odot$; escape velocity at $r = 0$ and initial recoiling velocity in $km\,s^{-1}$; initial Mach number M; mass deficit in stars, gas and their sum in units of M_{BH}; core radius in unit of scale radius, a; mass of particles initially bound to the BH $M_{gas,b}$ in units of M_{BH}. Runs g and H correspond to the case of instantaneous removal of the BH. In runs a, b, g (C, D, E, F, H), the scale radius is equal to 4 (8) kpc and the initial sound speed is 400 (300) $km\,s^{-1}$.

Run	M_{BH}	v_{esc}	v_{rec}	M	$M_{def,star}/M_{BH}$	$M_{def,gas}/M_{BH}$	$M_{def,tot}/M_{BH}$	r_{core}/a	$M_{gas,b}/M_{BH}$
a	2	1490	500	1.3	1	0.24	1.24	0.16	0.13
b	2	1490	1200	3	3.2	0.63	3.83	0.35	0.01
C	6	1054	400	1.3	1.8	0.19	2.	0.16	0.3
D	6	1054	700	2.3	3.5	0.35	3.85	0.275	0.1
E	6	1054	900	3	3.8	0.43	4.2	0.36	0.061
F	6	1054	1000	3.3	4.	0.53	4.5	0.41	0.05
g	2	1490	∞	∞	0.73	0.06	0.79	0.075	–
H	6	1054	∞	∞	1.53	0.21	1.75	0.19	–

model for 1 Gyr to verify its stability. After the ejection, we halt our simulations when the BH has settled into its Brownian motion.

We explore the ejection of the BH for different recoil velocities v_{rec} ranging from 0.2 to 0.95 the escape velocity, v_{esc}. In the simulations with $a = 4$ (8) kpc, the escape velocity at $r = 0$ is 1490 (1054) $km\,s^{-1}$ and the central initial sound speed is 400 (300) $km\ s^{-1}$. The resulting initial Mach number, defined as $\mathcal{M} \equiv v_{rec}/c_{s,0}$, ranges between 1 and 3.3. Table 1 lists physical parameters for all eight models: a through H. We will identify the runs referring to the light (heavy) BH with lowercase (uppercase) letters.

3 BLACK HOLE INTERACTION WITH THE HOT GAS

The recoiling BH reaches its first apocentre $r_{apo} \sim a[(1 - v_{rec}^2/v_{esc}^2)^{-1} - 1]$. Following the kick, the motion of the BH exhibits three distinct phases: (i) a decaying oscillatory radial motion guided by dynamical friction; (ii) a phase characterized by BH oscillations well inside the galaxy scale radius followed by (iii) the Brownian motion. These phases agree with what Gualandris & Merritt (2008) found for the collisionless case.

In the following, we investigate the direct influence that the ejection of the BH has on gas density and temperature, looking at the evolution of both radial profiles and two-dimensional maps.

3.1 Density and temperature radial profiles

We now turn our attention to the global disturbance that the BH imprints on the gas. We first focus on a simulation with $M_{BH} = 2 \times 10^9\,M_\odot$ (run b, $\mathcal{M} = 3$), and analyse how the density and temperature profiles change during the entire run. In run b, the orbit decays into the Brownian regime after ∼458 Myr (i.e. $\sim 20\,t_{dyn}$, where $t_{dyn} = [3\pi^2 a^3/(GM_{tot})^{1/2}]$.

Fig. 1 shows the evolution of the radial density profile. When the BH is at its first apocentre (22 Myr after the ejection), the central density drops creating a core within $\approx 2\,r_{inf}$. The density keeps decreasing until the BH sets into its Brownian motion. The final central gas density is ≈9– 10 times lower than the initial value, and the final gaseous core has a size $\approx 4\,r_{inf}$.

The evolution of the radial density profile is caused by the same two processes outlined by Boylan-Kolchin et al. (2004) and Merritt et al. (2004) for the stellar component. At first, the density drop is due to the sudden removal of the BH gravitational field and not to dynamical friction: in response to this change, the stellar and

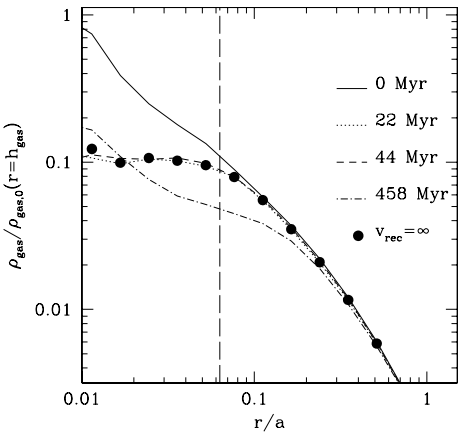

Figure 1. Radial density profiles of gas, in units of the initial central density at the softening radius, as a function of the distance from the centre of the galaxy in units of a for run b at different times. Solid line refers to the initial condition, dotted and dashed lines to the time at which the BH is at its first apocentre and first pericentre, respectively. Dot–dashed line refers to the final configuration when the BH orbit has decayed. Vertical line indicates the position of r_{inf}. Red dots refer to the run g where the BH has been instantaneously removed.

gaseous components readjust to a dynamical equilibrium state with no BH. To check this hypothesis, we carried out a test simulation where the BH was removed instantaneously from the galaxy (run g for $M_{BH} = 2 \times 10^9\,M_\odot$), and let the system evolve for 22 Myr. Density profiles for runs b and g at this time are indeed very similar, confirming this initial hypothesis. At later times, the density evolution is driven by dynamical friction, which injects energy into the background at each supersonic pericentric passage. When the orbital decay is completed, the combined action of the two processes ends with an erosion extending all the way to $4r_{inf}$.

Fig. 2 shows the evolution of the temperature profile in run b. The central temperature T decreases in response to the ejection of the BH as well. However, when the BH settles down in its Brownian motion, T returns to its virial value.

The final gas density profiles normalized to the initial profiles are shown in Fig. 3 for cases from a through F. Core formation occurs in all cases. For a fixed M_{BH}, the importance of the core increases with v_{rec}, while for a fixed v_{rec} it increases for more massive BHs, i.e. with the kinetic energy deposited by the BH. For low recoil velocities ($\mathcal{M} \sim 1$), the kinetic energy carried by the BH and deposited in its transit across the centre of the galaxy is low, and

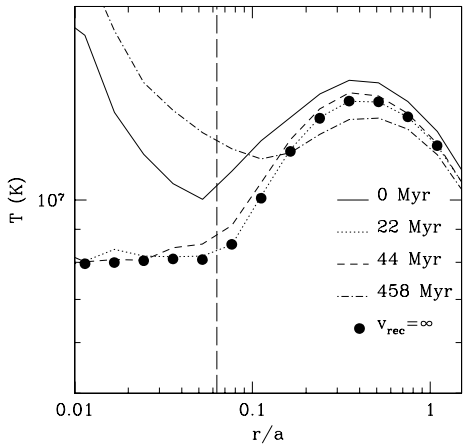

Figure 2. Radial temperature profiles of gas as a function of the distance from the centre of the galaxy in units of a for run b at different times. Solid line refers to the initial condition, dotted and dashed lines refer to the first apocentre and pericentre, respectively. Dot–dashed line refers to the final configuration. Vertical line indicates the position of $r_{\rm inf}$.

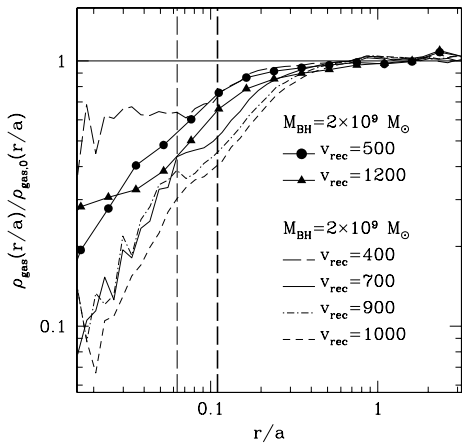

Figure 3. Final gas density profiles $\rho_{\rm gas}$ as function of r/a, normalized to the density profile at $t = 0$ $\rho_{\rm gas,0}$ for the two sets of run with different BH masses and recoil velocities $v_{\rm rec}$ (in units of km s^{-1}). Vertical lines refer to the influence radii of the two BH masses: light (heavy) curve for $M_{\rm BH} = 2\ (6) \times 10^9\,{\rm M}_\odot$.

the major perturbation acting on the gas is related to the temporary removal of the BH at the time of coalescence.

We compute final core radii and mass deficits for both the gaseous ($M_{\rm def,gas}$) and stellar ($M_{\rm def,star}$) components (see Table 1). $M_{\rm def,star}$ is always larger than $M_{\rm def,gas}$, because in all our simulations the stellar mass is larger as compared to the gaseous one. The total, star + gas, deficits span from 1.5 up to 4 $M_{\rm BH}$, in agreement with the results from collisionless simulations (Boylan-Kolchin et al. 2004; Merritt et al. 2004; Gualandris & Merritt 2007).

3.2 Density and temperature two-dimensional maps

In this section, we study the shape and extent of the density and temperature perturbations that the BH excites along its trail. We first discuss models with $\mathcal{M} \simeq 1$, i.e. runs a and C. During the orbital decay, the BH is always surrounded by a hot spherical overdensity of gaseous particles. The size of the spherical overdensity corresponds roughly to $r_{\rm b} \equiv GM_{\rm BH}/v_{\rm rec}^2$, i.e. the radius within which particles

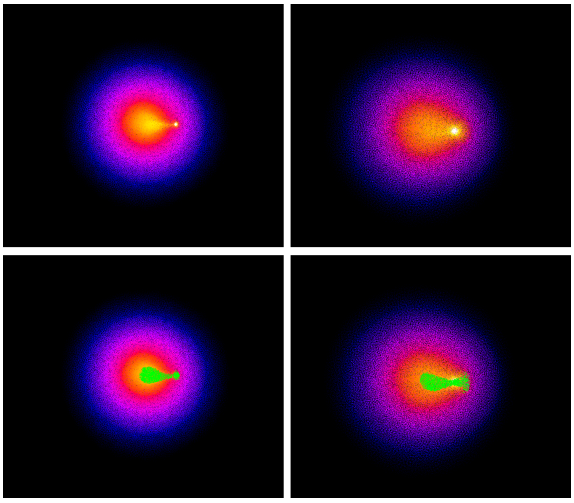

Figure 4. Upper panel: colour-coded gaseous density maps in logarithmic scale for runs a (left-hand panel) and C (right-hand panel) ($v_{\rm rec} = 500$ and 400 km s^{-1}, respectively) when the BH is at its first apocentre. Brighter colours refer to higher densities that range between 0.1 and 10^{-3} cm^{-3}. Lower panel: same maps but where the gaseous particles initially bound to the BH are marked in green. Boxes are 2 a on a side (i.e. 8 and 16 kpc for runs a and C, respectively). The BH initial orbit is on the x-axis and maps are projected in the x–y plane.

remain bound after the BH is kicked. The density enhancement is illustrated in the upper panels of Fig. 4 for both runs when the BH is at its first apocentre.

Another characteristic feature in the density maps of these early dynamical phases is a stream of gas particles lagging behind the BH trail. We argue that this gas is a stripped material initially residing inside $r_{\rm inf}$. To test this hypothesis we mark, at the start of runs a and C, the particles gravitationally bound to the BH,[1] and then follow their dynamics. Fig. 4 shows the density map of the gas surrounding the BH at its first apocentre. In the lower panels, the particles originally bound to the BH are marked in green. Here, a clear spatial coincidence between the stream and the marked particles appears, thus supporting our hypothesis.

As we move to higher velocities ($\mathcal{M} > 2$), the mass of particles initially bound to the recoiling BH ($M_{\rm gas,b}$) decreases considerably as reported in Table 1. Again, this was previously noted for the stellar case by Gualandris & Merritt (2008). The quasi-spherical swarm of hot gaseous particles around the BH becomes less relevant, and for the case with the highest speed (runs b and F), it is no longer visible even soon after the ejection. The lack of particles around the BH for large Mach numbers is a consequence of our resolution limits: for kick velocities $\gtrsim$800 km s^{-1} (700 km s^{-1}) and for the light (heavy) BH, the radius $r_{\rm b}$ drops below our resolution limit so that we are unable to resolve the initially bound particles anymore.

New features appear when $\mathcal{M} > 2$ initially: a steep, conical overdensity develops, i.e. a Mach cone becomes visible in the density maps, as shown in Fig. 5. The opening angle of the cone is inversely proportional to $\mathcal{M}$, and varies along the BH trajectory as both its speed and background temperature vary. The shape of the cone is sharpest at the first pericentre passage, where the contrast between

[1] We define particles gravitationally bound to the BH as done in Gualandris & Merritt (2008): we calculate the relative energy between the BH and each particle. When this energy is negative, we define the particle as bound to the BH.

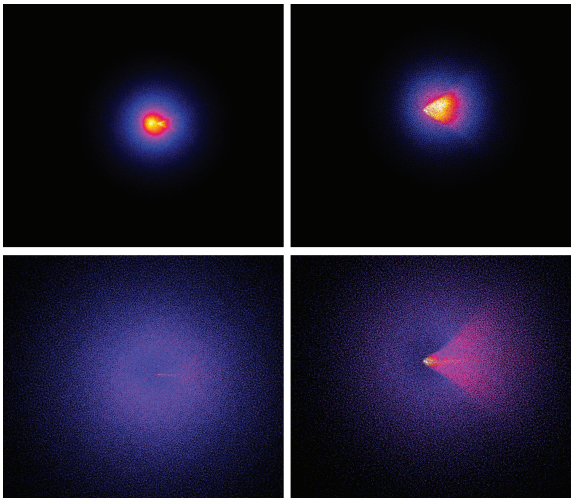

Figure 5. Upper panel: colour-coded gaseous density maps in linear scale for run b (left-hand panel) and E (right-hand panel) with $\mathcal{M} = 3$ when the BH is at its first pericentre. Density range between 0.001 and 0.05 cm^{-3} q. Lower panel: colour-coded temperature map in logarithmic scale between 5×10^6 and 1.5×10^7 K. Boxes are 4 and 20 kpc on a side for runs b and E, respectively. The BH initial orbit is on the x-axis and maps are projected in the x–y plane.

the speed of the perturber and the temperature of the gas is the highest (see Fig. 2). The cone then weakens during the rest of the simulation as dynamical friction slows down the BH motion, and the temperature returns to its virial value. The Mach cone is clearly visible along the direction orthogonal to the BH velocity vector, and it can still be recognizable as long as the angle between the line of sight and the BH is below $\sim 45^\circ$.

All these features are transient and have a characteristic lifetime that depends on the BH–galaxy mass ratio, on the extent of the recoil velocity imparted at the moment of BH coalescence and on the background. For low Mach numbers, $\mathcal{M} \sim 1$, the overdensity around the BH is more easily visible when the BH is at apocentre as the density and temperature contrast with the background are the highest. As the BH spends most of the time at apocentre, this overdensity can be observed for 10–100 Myr. For high Mach numbers, i.e. recoil velocities near escape, the Mach cone becomes the main feature, and it is seen during the first supersonic pericentres close to the central region of the host galaxy, within a scale ranging between 0.5 and 2 kpc. The corresponding lifetime is a few tens of Myr.

3.3 Gas fraction

We now briefly discuss how the density and temperature perturbations excited by the BH travelling across the hot gas of the galaxy depend on the fraction of gas $f_{\rm gas}$ relative to the stellar mass. Although we have modelled gas-rich early-type galaxies with $f_{\rm gas} = 0.1$, the dynamical evolution of the BH is still dominated by the stellar component. As a consequence, a further reduction of $f_{\rm gas}$ does not alter the BH orbit or the characteristic decay time. As the gas is in virial equilibrium, its sound speed and temperature are determined by the overall gravitational potential, and thus do not vary for smaller $f_{\rm gas}$. Since the shape of the perturbation depends on the value of the Mach number and on the size of the BH influence radius, galaxy models with different gas fractions but same $\mathcal{M}$ and $M_{\rm BH}$ differ only in the total X-ray luminosity (discussed in Section 4). We run a test simulation with $f_{\rm gas} = 0.01$, $\mathcal{M} = 2.3$ and $M_{\rm BH} = 6 \times 10^9$ M$_\odot$ to verify these scaling and find good agreement with our expectations.

4 DETECTABILITY

The motion of the BH perturbs the density and temperature distribution. The bremsstrahlung emission from the perturbed gas is expected to create X-ray features above the diffuse emission from the underlying hot gas in the galaxy. In this section, we quantify the detectability of signatures related to recoiling BHs in X-rays. We create synthetic *Chandra* observations using the code X-ray MAp Simulator (Gardini et al. 2004; Rasia et al. 2008). The mock event files are generated in the soft band [0.7, 2] keV, assuming the response matrix file and the ancillary response file of the *Chandra* detector ACIS-S 3. The images are created assuming an exposure time of 10 ks for the heavy BH and 100 ks for the light BH. The galaxy–BH system is considered to be at the distance of Virgo (z = 0.004), meaning that the field of view of our detector (8.3 arcmin) corresponds to 42 kpc. The orbital plane of the BH is perpendicular to the X-ray image and oriented along the horizontal axis unless otherwise noted.

The drop in central density is less dramatic for the light BH and the swarm of bound particles less evident. The X-ray contrast of the features produced over the underlying galaxy is consequently weaker than in runs with a heavy BH. Identification of recoil signatures on raw surface brightness maps is hard. To better highlight the influence of the BH in *Chandra* maps and to quantify its relevance over the background galaxy, we create 'mirror images'. We rotate a galaxy image by 180° around the axis orthogonal to the BH motion, and then divide the original image by the rotated one (this technique is reminiscent of the 'Asymmetry' index used in optical astronomy, e.g. Conselice 2003).

Selected *mirror images* for the light BH are shown in Fig. 6. When $\mathcal{M} = 1$ (run a), the perturbation of the gas results in an X-ray enhancement offset relative to the galaxy centre. Its concentration and spherical shape can be associated with the feature outlined in

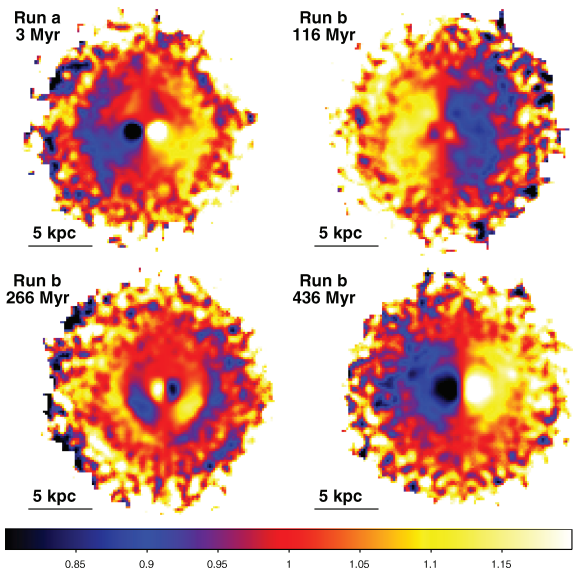

Figure 6. Mirror images for the light BH smoothed with a Gaussian filter. Top-left panel: run a, when the BH is in its first apocentre. Top-right, bottom-left and bottom-right panels: mirror images for run b at three different moments of the BH motion (time after the ejection is shown in each panel). The colour scale is linear between 0.8 and 1.2.

Fig. 4. The three images for run b represent three different moments of the BH orbital decay. During the first oscillations, the BH has an orbit with large radii (∼8 kpc). The residues of its passage are visible, as broad wings, up to 5 kpc from the centre. As the decay proceeds the orbital radius decreases and in this particular simulation the BH starts to precess after ∼200 Myr. The second mirror image is taken after 266 Myr when the motion axis is tilted by almost 45° respect to its original orientation. Here, the BH motion is traced by the two yellow spots oriented along the BH trajectory. The last image refers to the last phase of the BH motion when the BH moves in a short orbit across the centre and passes frequently through the same excited region. The X-ray enhancement increases the background emission by 30 per cent.

4.1 Detectability of 'outliers'

As already mentioned, the heavier the BH with respect to its host, the stronger the thermodynamical perturbations are. We recall that 'heavy' in this context means that the BH is above the $M_{\rm BH} - M_{\rm bulge}$ relation (i.e. an 'outlier').

A heavier BH perturbs the background more strongly. Fig. 7 shows photon images of the X-ray emission detectable by *Chandra* for run D. In this case, the presence of the BH results not only as a clear distortion of the isophotal contours, but also as a peaked emission separate from the centre. This spherical X-ray enhancement survives for many passages through the centre. In Fig. 8, we clearly distinguish the strong feature of the Mach cone for run E. The mirror images, in this case, present sharp well-defined edges limiting the Mach cone which reaches a maximum contrast of 300 per cent over the background. The first panel shows the X-ray images when the cone axis is aligned with the horizontal axis. It is important to assess if the features are visible along lines of sight not exactly orthogonal to the BH motion. We produce maps where the angle between the cone axis and the plane orthogonal to the line of sight increases from 0° (the reference value) to 60° in steps of 5°. The signature is recognizable as a cone when the angle is below

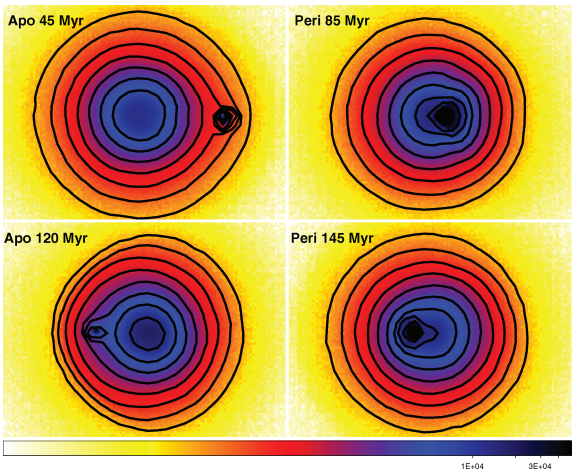

Figure 7. Simulated colour-coded maps of the X-ray emission detectable by *Chandra* (ACIS-S3 chip) for run D. The photon images are computed in the [0.7 2] keV band, background subtracted and 1 arcsec binned. The angular size is 2.7 arcmin corresponding approximately at 14 kpc at the source redshift ($z = 0.004$). The scale is logarithmic and the isophotal contours (shown in black) are logarithmically equi-spaced between 100 and 50 000. Different panels correspond to first apocentric phases (denoted by Apo) and pericentric ones (denoted by Peri). The last pericentre showed is after 145 Myr, while the last apocentre is at 120 Myr.

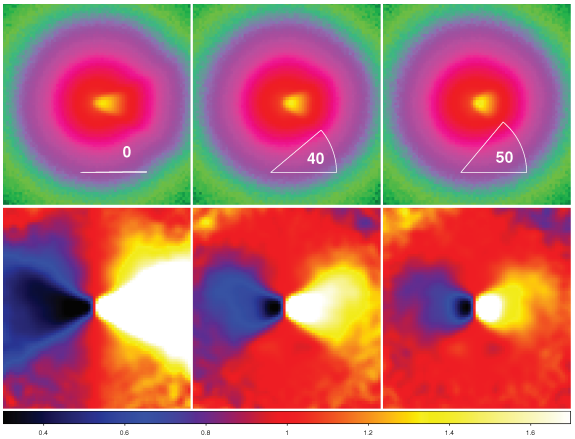

Figure 8. Upper panels: simulated colour-coded maps of the X-ray emission detectable by *Chandra* (ACIS-S3 chip) for run E for different angles (reported in each image) between the plane orthogonal to the line of sight and the BH motion. Lower panels: mirror images for run E (with the heavy BH) smoothed with a Gaussian filter for different rotation angles between the line of sight and the BH motion. The colour scale is linear between 0.3 and 1.8. The angular size in all images is 2 arcmin corresponding approximately at 10 kpc at the source redshift ($z = 0.004$).

45°, in good agreement with the result we found for the density two-dimensional maps alone. For angle above 45°, we still detect a strong inhomogeneity but the cone structure is lost.

Chandra can resolve the wake of 'outliers' to a greater distance and in smaller galaxies. The Mach cone is not only a key feature for revealing a moving BH with high recoil velocities, but it also highlights the presence of an outlier. In the following, we rescale our results to galaxies with smaller gas fraction and to smaller galaxies, in both cases hosting massive BHs above the $M_{\rm BH} - M_{\rm bulge}$ relation, 'outliers'.

We first consider how the observability of the conical wake depends on the gas fraction. As discussed above, the dynamical evolution of the BH is mainly driven by the interaction with stars, so that the shape of the X-ray features is a function only of the properties of the recoiling BH. In galaxies with a smaller gas fraction, it is only the total X-ray flux that changes.

In order to determine if the wake is visible relative to the background galaxy, the corresponding signal-to-noise[2] ratio (S/N) needs to be greater than a given detectability threshold. The counts expected from a *Chandra* observation of 10 ks give values of the S/N greater than 10 for gas fractions above $f_{\rm gas} = 10^{-3}$, reassuring that, at the distance of Virgo, $\sim 10^9\,{\rm M}_\odot$ BHs ejected with supersonic velocity are all detectable.

We now consider the sensitivity of our results to the size of the galaxy. Our simulations are scale-free, as long as the units we use are consistent with the same gravitational constant adopted in GADGET to evolve the system. If we scale the masses ($M' = \alpha M$), the radii need to be rescaled ($R' = \alpha^{0.56} R$; see Shen et al. 2003) in order to preserve the relationship between the scale radius and the mass of the galaxy: accordingly the time follows $t' = \alpha^{0.34} t$. For the new system, the luminosity of the bremsstrahlung emission is related to the old one by $L' = \alpha^{0.54} L$.

In order to determine the minimum value of α for which we can still observe the wake, we have to take into account not only the S/N,

[2] Note that in this case the noise is given by the emission of the host galaxy itself.

but also the angular resolution of *Chandra*. For our reference galaxy, the maximum radius of the wake in run b at the first pericentre is ≈2 kpc. We consider the wake in a galaxy at a distance d as resolved by *Chandra* if the angular extent of the wake is covered by four resolution elements (0.5 arcsec, i.e. the angular resolution of the telescope). For galaxies at distances comparable the Virgo cluster the critical α for a wake to be resolved is $\alpha_{\rm lim} \sim 8 \times 10^{-3}$, corresponding to a BH mass greater than $\sim 5 \times 10^7\,{\rm M}_\odot$. Fixing $\alpha_{\rm lim}$, we have carried on the same analysis outlined above for $f_{\rm gas} = 0.1$, 10^{-2} and 10^{-3}. For $f_{\rm gas} = 0.1$ and 10^{-2}, the S/N is again greater than 10. For $f_{\rm gas} = 10^{-3}$, it drops to 2 only.

What happens if we consider more distant galaxies? The resolution of *Chandra* would allow us to resolve the wake in our reference galaxy up to a distance of ∼300 Mpc. The minimum value of α is related to the distance d by $\alpha \sim 8 \times 10^{-3}\,(d/20\,{\rm Mpc})^{1/0.56}$. The detection limits imposed by the S/N are less tight than those given by the requirement on the spatial resolution unless $f_{\rm gas} < 10^{-2}$.

5 SUMMARY AND DISCUSSION

In this paper, we studied the perturbation that a recoiling massive BH can imprint on the hot gaseous component of its host elliptical. The BH is able to affect not only the stellar component (as previously noted by Boylan-Kolchin et al. 2004 and Gualandris & Merritt 2008), but also the gaseous one. Indeed the ejection of the central object perturbs the gas in both its equilibrium properties and along its trail.

The BH triggers the formation of a density core on the scale of a few $r_{\rm inf}$, resulting from its sudden removal at the time of its ejection and from the kinetic energy deposition that continue eroding the central density over the whole orbital decay. Along its path, the BH imprints in the gas peculiar features that help to reveal its presence while travelling across its host. The strength of these features depends not only on the ejection velocity, but also on the BH mass and thus on the relationship between a hole and its host. When the motion is subsonic, the BH is surrounded by a nearly spherical distribution of gas particles, resulting in an enhancement of the underlying bremsstrahlung X-ray emission. For the lighter BH (on the $M_{\rm BH} - M_{\rm bulge}$ relation), the X-ray feature is visible out to the distance of Virgo. When the motion is supersonic, the BH shocks the gas exciting a conical density and temperature perturbation (the Mach cone), but the enhancement does not lead to a detectable X-ray signal. By contrast, an exceptionally massive BH (above the $M_{\rm BH} - M_{\rm bulge}$ relation) carries features that are not only more intense and more detectable in a larger cosmic volume, but that also have a unique flavour: the Mach cone is clearly recognizable in X-ray maps with an increase in surface brightness by a factor of 2 to 3 over the background. Therefore, detection of the Mach cone becomes of twofold importance: (i) as a probe of high-velocity recoils and (ii) as an assessment of the scatter of the $M_{\rm BH} - M_{\rm bulge}$ relation at large BH masses. The different shapes in the disturbance can thus, in principle, help in constraining the extent of the gravitational wave recoil and the scatter in scale relationship between BH masses and their hosts.

The lifetime of the different features correlates with their shape. For initially low Mach numbers, the spherical overdensity surrounding the BH appears at every apocentre (i.e. where the BH resides most) where the density contrast is the highest. This signature lasts up to 100 Myr. For initially high Mach numbers, the Mach cone, recognizable during supersonic passages through the centre, is shorter lived. Despite its longer duration, the subsonic modes carry less information as it can be created either by an initially fast-moving BH once its orbit has decayed, or by an initially slow BH.

It is important to note that the X-ray features recognized in this work are not due to the direct emission from the BH but only due to the perturbed large-scale hot gas of the underlying galaxy. In addition to this, the BH itself can produce its own optical and X-ray emission if it is able to retain a punctured accretion disc at the moment of its ejection from the centre, as suggested by Loeb (2007) (and studied in a statistical context by Volonteri & Madau 2008). The kicked BH in this case can turn on as a displaced quasi-stellar object (QSO)/active galactic nuclei, and a key manifestation of a large recoil should be imprinted in the line systems shifted in velocity from the host galaxies (Bonning, Shields & Salviander 2007). This off-nuclear QSO emission can coexist with the large-scale emission features studied in this paper. The contemporary observation of a set of offset lines and a Mach cone can potentially provide information on the tangential and radial velocities resulting from the kick. Off-centred flares occurring from tidal disruption of bound stars or from marginally bound gas that infall on the disc can also be present during the lifetime of the recoiling BH (Merritt, Schnittman & Komossa 2008; O'Leary & Loeb 2008; Shields & Bonning 2008).

The electromagnetic signature of a recoiling BH, detailed in this paper, is different from the one expected in the immediate vicinity of a coalescence event. Electromagnetic afterglows of *LISA* coalescence events (Milosavljević & Phinney 2005; Dotti et al. 2006; Kocsis & Loeb 2008; Lippai, Frei & Haiman 2008) have peculiar off–on time-dependent features varying on much shorter times and spatial scales.

The detectability of X-ray features favours heavier BHs as the strength of the perturbation increases with $M_{\rm BH}$. Accordingly, the observability is strongly biased towards more massive ellipticals. Interestingly, these massive BHs are out of the *LISA* frequency sensitivity, so that this study would complement our knowledge of gravitational wave in-spiral events in a window not accessible to *LISA*. Massive ellipticals could be the preferred sites where coalescing BHs are expected to get the largest kick ever, due to the lack of a mechanism able to align the two spins prior to the merger (Bogdanović, Reynolds & Miller 2007). The discovery of a prominent X-ray feature in the form of a Mach cone will, in principle, support the idea that high-velocity recoils are allowed in environments where a cool dissipative gaseous component is absent.

ACKNOWLEDGMENTS

We wish to thank Stuart Shapiro and Martin Elvis for fostering the research that led to this paper, and Renato Dupke and Lea Giordano for useful discussions. MV and ER acknowledge support from NASA under the *Chandra* award GO7-8138C and through *Chandra* Postdoctoral Fellowship grant number PF6-70042 awarded by the *Chandra* X-ray Center, which is operated by the Smithsonian Astrophysical Observatory for NASA under contract NAS8-03060. BD and MD thank Luca Paredi for technical support. Simulations were performed on the Yoda cluster at the University of Como. BD thanks the Astronomy Department of University of Michigan for the hospitality, and MC thanks the hospitality of the Aspen Center for Physics, where part of the study was discussed.

REFERENCES

Armitage P. J., Natarajan P., 2002, ApJ, 567, L9

Baker J. G., Boggs W. D., Centrella J., Kelly B. J., McWilliams S. T., Miller M. C., van Meter J. R., 2007, ApJ, 668, 1140

Baker J. G., Boggs W. D., Centrella J., Kelly B. J., McWilliams S. T., Miller M. C., van Meter J. R., 2008, ApJ, 682, L29
Berczik P., Merritt D., Spurzem R., Bischof H.-P., 2006, ApJ, 624, L21
Bogdanović T., Reynolds C. S., Miller M. C., 2007, ApJ, 661, L147
Bonning E. W., Shields G. A., Salviander S., 2007, ApJ, 666, L13
Boylan-Kolchin M., Ma C.-P., Quataert E., 2004, ApJ, 613, L37
Bruegmann B., Gonzalez J., Hannam M., Husa S., Sperhake U., 2008, Phys. Rev. D, 77, 124047
Campanelli M., Lousto C., Zlochower Y., Merritt D., 2007a, ApJ, 659, L5
Campanelli M., Lousto C. O., Zlochower Y., Merritt, D., 2007b, Phys. Rev. Lett., 98, 231102
Conselice C. J., 2003, ApJS, 147, 1
Decarli R., Gavazzi G., Arosio I., Cortese L., Boselli A., Bonfanti C., Colpi M., 2007, MNRAS, 381, 136
Dotti M., Colpi M., Haardt F., 2006, MNRAS, 367, 103
Dotti M., Salvaterra R., Sesana A., Colpi M., Haardt F., 2006, MNRAS, 372, 869
Dotti M., Colpi M., Haardt F., Mayer L., 2007, MNRAS, 379, 956
Escala A., Larson R. B., Coppi P. S., Mardones D., 2004, ApJ, 607, 765
Escala A., Larson R. B., Coppi P. S., Mardones D., 2005, ApJ, 630, 152
Favata M., Hughes S. A., Holz D. E., 2004, ApJ, 607, L5
Ferrarese L., Merritt D., 2000, ApJ, 539, L9
Gardini A., Rasia E., Mazzotta P., Tormen G., De Grandi S., Moscardini L., 2004, MNRAS, 351, 505
Gebhardt K. et al., 2000, ApJ, 539, L13
Gualandris A., Merritt D., 2008, ApJ, 678, 780
Häring N., Rix H. W., 2004, ApJL, 604, L89
Hernquist L., 1990, ApJ, 356, 359
Hernquist L., 1993, ApJS, 86, 389
Herrmann F., Hinder I., Shoemaker D. M., Laguna P., Matzner R. A., 2007a, Phys. Rev. D, 76, 084032
Herrmann F., Hinder I., Shoemaker D., Laguna P., 2007b, Class. Quantum Gravity, 24, 33
Herrmann F., Hinder I., Shoemaker D., Laguna P., Matzner R. A., 2007c, ApJ, 661, 430
Hopkins P. F., Hernquist L., Cox T. J., Di Matteo T., Robertson B., Springel V., 2006, ApJS, 163, 1
Hudson D. S., Reiprich T. H., Clarke T. E., Sarazin C. L., 2006, A&A, 453, 433
Kocsis B., Loeb A., 2008, Phys. Rev. Lett., 101, 041101
Koppitz M., Pollney D., Reisswig C., Rezzolla L., Thornburg J., Diener P., Schnetter E., 2007, Phys. Rev. Lett., 99, 041102
Lauer T. R. et al., 2007, ApJ, 662, 808
Lippai Z., Frei Z., Haiman Z., 2008, ApJL, 676, L5
Loeb A., 2007, Phys. Rev. Lett., 99, 041103
Mayer L., Kazantzidis S., Madau P., Colpi M., Quinn T., Wadsley J., 2007, Sci, 316, 1874
Merritt D., Milosavljević M., 2005, Living Reviews in Relativity, 8, 8
Merritt D., Milosavljević M., Favata M., Hughes S. A., Holz D. E., 2004, ApJ, 607, L9
Merritt D., Schnittman J. D., Komossa S., 2008, preprint (arXiv:0809.5046)
Milosavljević M., Merritt D., 2001, ApJ, 563, 34
Milosavljević M., Phinney E. S., 2005, ApJ, 622, L93
O'Leary R. M., Loeb A., 2008, preprint (arXiv:0809.4262)
Owen F. N., Odea C. P., Inoue M., Eilek J. A., 1985, ApJ, 294, L85
Pretorius F., 2007, preprint (arXiv:0710.1338)
Rasia E., Mazzotta P., Bourdin H., Borgani S., Tornatore L., Ettori S., Dolag K., Moscardini L., 2008, ApJ, 674, 728
Richstone D. et al., 1998, Nat, 395, A14
Rodriguez C., Taylor G. B., Zavala R. T., Peck A. B., Pollack L. K., Romani R. W., 2006, ApJ, 646, 49
Schnittman J. D., Buonanno A., 2007, ApJ, 662, L63
Sesana A., Haardt F., Madau P., 2007, ApJ, 660, 546
Shen S., Mo H. J., White S. D. M., Blanton M. R., Kauffmann G., Voges W., Brinkmann J., Csabai I., 2003, MNRAS, 343, 978
Shields G. A., Bonning E. W., 2008, ApJ, 682, 758
Springel V., Yoshida N., White S. D. M., 2001, New Astron., 6, 79
Tundo E., Bernardi M., Hyde J. B., Sheth R. K., Pizzella A., 2007, ApJ, 663, 53
Volonteri M., Madau P., 2008, ApJ, 687, L57
Volonteri M., Haardt F., Madau P., 2003, ApJ, 582, 559
Yu Q., 2002, MNRAS, 331, 931

This paper has been typeset from a TEX/LATEX file prepared by the author.